Neurosci. Bull. July, 2021, 37(7):921–933
https://doi.org/10.1007/s12264-021-00697-6

www.neurosci.cn
www.springer.com/12264

ORIGINAL ARTICLE

CCL2/CCR2 Contributes to the Altered Excitatory-inhibitory Synaptic Balance in the Nucleus Accumbens Shell Following Peripheral Nerve Injury-induced Neuropathic Pain

Xiao-Bo Wu[1] · Qian Zhu[1] · Yong-Jing Gao[1,2]

Received: 17 July 2020 / Accepted: 10 February 2021 / Published online: 18 May 2021

Abstract The medium spiny neurons (MSNs) in the nucleus accumbens (NAc) integrate excitatory and inhibitory synaptic inputs and gate motivational and emotional behavior output. Here we report that the relative intensity of excitatory and inhibitory synaptic inputs to MSNs of the NAc shell was decreased in mice with neuropathic pain induced by spinal nerve ligation (SNL). SNL increased the frequency, but not the amplitude of spontaneous inhibitory postsynaptic currents (sIPSCs), and decreased both the frequency and amplitude of spontaneous excitatory postsynaptic currents (sEPSCs) in the MSNs. SNL also decreased the paired-pulse ratio (PPR) of evoked IPSCs but increased the PPR of evoked EPSCs. Moreover, acute bath application of C–C motif chemokine ligand 2 (CCL2) increased the frequency and amplitude of sIPSCs and sEPSCs in the MSNs, and especially strengthened the amplitude of N-methyl-D-aspartate receptor (NMDAR)-mediated miniature EPSCs. Further *Ccl2* overexpression in the NAc *in vivo* decreased the peak amplitude of the sEPSC/sIPSC ratio. Finally, *Ccr2* knock-down improved the impaired induction of NMDAR-dependent long-term depression (LTD) in the NAc after SNL. These results suggest that CCL2/CCR2 signaling plays a role in the integration of excitatory/inhibitory synaptic transmission and leads to an increase of the LTD induction threshold at the synapses of MSNs during neuropathic pain.

Keywords E/I balance · Synaptic transmission · LTD · CCL2 · CCR2 · Nucleus accumbens · Neuropathic pain

Introduction

The nucleus accumbens (NAc) plays a critical role in mediating reward, motivation, depression, and chronic pain. Medium spiny neurons (MSNs), the main projection neurons in the NAc, are involved in a decrease of motivation under chronic pain conditions [1], as well as an increase of pain sensitivity and the induction of depression after nerve injury [2, 3]. Interrupting the activity of the MSNs in the medial shell of the NAc relieves peripheral nerve injury-induced neuropathic pain in rats [4]. Electrophysiological studies have shown that nerve injury changes the excitatory glutamatergic transmission at synapses of MSNs in the NAc [1, 2], manifested as a decreased ratio of α-amino-3-hydroxy-5-methyl-4-isoxazolepropionic acid receptor (AMPAR)- to N-methyl-D-aspartate receptor (NMDAR)-mediated currents [1] and changes in the function of specific AMPAR and NMDAR subunits [1, 5]. Accordingly, the expression levels of the GluA1 subunit of the AMPAR and the GluN2B subunit of the NMDAR are increased on the postsynaptic membrane surface in MSNs of the NAc under neuropathic pain conditions [1, 5–7]. Although chronic pain-induced neural adaptations at excitatory glutamatergic synapses have been investigated, little is known about how inhibitory synaptic input to MSNs of the NAc is affected during neuropathic pain.

✉ Xiao-Bo Wu
xbwu1983@ntu.edu.cn

✉ Yong-Jing Gao
gaoyongjing@ntu.edu.cn; gaoyongjing@hotmail.com

[1] Institute of Pain Medicine and Special Environmental Medicine, Nantong University, Nantong 226019, China

[2] Co-innovation Center of Neuroregeneration, Nantong University, Nantong 226001, China

The MSNs integrate GABAergic inhibitory synaptic inputs from intrinsic and extrinsic sources [8, 9]. Finely-tuned excitatory and inhibitory synaptic transmission to a neuron regulates the functional state for action potential discharge and gates synaptic plasticity [10–12]. It has been demonstrated that impaired excitatory/inhibitory (E/I) balance in the spinal cord contributes to central sensitization and chronic pain [12]. In the brain, disruption of the E/I balance in the somatosensory cortex is linked to large-scale neuronal plasticity and pain sensitivity in mice with multiple sclerosis [13]. More recent evidence has shown that nerve injury attenuates the overall E/I balance of basolateral amygdala inputs to prefrontal cortex neurons [14]. The NAc shell plays an important role in mediating neuropathic pain [2, 15]. Whether the E/I synaptic balance in the MSNs of NAc shell is altered under neuropathic pain condition deserves investigation.

Chemokine CCL2 (also called monocyte chemoattractant protein 1) and its receptor CCR2 are involved in the pathogenesis of neuropathic pain *via* increasing glutamatergic synaptic transmission in the spinal cord [16]. In addition, our recent study showed that peripheral nerve injury increases the expression of CCL2 and CCR2 in the MSNs of the NAc shell. Importantly, inhibition of CCR2 in the NAc shell by shRNA or an antagonist attenuates spinal nerve ligation (SNL)-induced neuropathic pain and the associated depressive behaviors in mice [3]. Consistent with this, overexpression of CCL2 in the NAc induces pain hypersensitivity and depression-like behaviors [3]. In addition, CCL2/CCR2 increases NMDAR-mediated currents in the cells *via* activating extracellular signaling-regulated kinase (ERK) [3, 17]. It has been reported that the enhanced function of NMDARs modulates the magnitude of long-term depression (LTD) induced by low-frequency stimulation (LFS) at MSN synapses in the NAc [18, 19]. Moreover, nerve injury- or inflammation-induced chronic pain attenuates and even impairs the induction of LTD in the anterior cingulate cortex [20, 21]. Whether CCL2/CCR2 signaling in the NAc shell regulates neuropathic pain and depression [3] *via* modulation of the E/I balance and NMDAR-mediated LTD remains unknown.

In the current study, we first assessed the impact of SNL on the excitatory-inhibitory current ratio at MSN synapses in the NAc shell and confirmed that the E/I balance was disrupted under SNL-induced neuropathic pain conditions. We also found that the increased CCL2/CCR2 in the NAc after SNL contributed to the disrupted E/I balance and NMDAR-mediated LTD in the NAc shell.

Materials and Methods

Animals and Surgery

Male ICR mice (8–12 weeks) were purchased from the Experimental Animal Center of Nantong University and housed in the Animal Facility of Nantong University. The SNL model was created as previously described [22]. Briefly, mice were anesthetized with 2% isoflurane and the bilateral L5 spinal nerves were exposed and ligated. For sham operation, the L5 spinal nerves were exposed but not ligated. All the procedures were approved by the Animal Care and Use Committee of Nantong University and performed in accordance with the institutional guidelines for the International Association for the Study of Pain.

Lentiviral Vector Construction and Intra-NAc Injection

The *Ccl2*-overexpression lentivirus *(*LV-*Ccl2)* and negative control lentivirus (LV-*NC*) were generated as described in our previous study [3]. In brief, recombinant lentivirus expressing *Ccl2* vector was designed by using the pGV365 lentiviral expression vector to generate pLV-Ubi-Ccl2-3FLAG-CMVEGFP (LV-*Ccl2*). A lentiviral vector that expressed GFP alone (LV-*NC*) was produced as control. In addition, shRNAs targeting the mice *Ccr2* and negative control (NC) were also designed as described previously [3]. The recombinant lentivirus shRNA-expressing vectors containing NC (LV-*NC*, scramble-shRNA) or *Ccr2* (LV-*Ccr2* shRNA, 5'-TGC ATT AAT CCT GTC ATT T-3') were constructed using pGCSIL-GFP vector by Shanghai GeneChem. To inject the lentivirus, mice were anesthetized using isoflurane. The head was fixed in a stereotaxic apparatus. Two holes were drilled on the skull (anteroposterior: bregma +1.53 mm, lateral: ±0.8 mm, depth: 4.82 mm). The lentivirus (0.25 μL per side) was injected into the NAc through a 32G needle (Hamilton) within 10 min. After the injection, the needle remained in the position for 5–6 min, and the scalp was sutured.

NAc Slice Preparation

NAc slices were prepared and patch-clamp recordings were made as previously described [3]. Briefly, each mouse was deeply anesthetized with 5% isoflurane and sacrificed 14 to 21 days after SNL or sham operation. The brain was quickly removed, and sagittal slices (300 μm) containing the NAc and prefrontal cortex were cut on a Vibratome (VT1000S; Leica, Germany) in sucrose-rich ice-cold artificial cerebrospinal fluid (aCSF) containing (in mmol/

L): 235 sucrose, 25 $NaHCO_3$, 2.5 KCl, 1.2 $CaCl_2$, 1.25 NaH_2PO_4, 2.5 $MgCl_2$, and 10 glucose (pH 7.2–7.4 when bubbled with 95% O_2 and 5% CO_2). Slices were incubated in normal aCSF (oxygenated with 95% O_2 and 5% CO_2) containing (in mmol/L): 125 NaCl, 1.25 NaH_2PO_4, 3 KCl, 1.2 $MgCl_2$, 2.4 $CaCl_2$, 26 $NaHCO_3$, and 11 glucose for 30 min at 34°C and subsequently kept at room temperature until transfer to the recording chamber.

Patch-clamp Recording from NAc Shell Slices

MSNs within the NAc shell were visualized under a BX51WI infrared-differential interference contrast microscope (Olympus, Japan). Patch-clamp recordings of inhibitory or excitatory postsynaptic currents (IPSC/EPSC) at synapses of NAc shell neurons were conducted with a patch-clamp amplifier (Multiclamp 700B; Axon Instruments, Burlingame, CA). Currents were filtered at 2 kHz and sampled at 10 kHz with a digitizer (DigiData 1440A; Axon Instruments). All recordings were analyzed using Clampfit 10.4 software (Molecular Devices, Sunnyvale, CA). MSNs in the NAc slice were identified by their small size (< 20 μm) and hyperpolarized resting membrane potential (– 75 to – 85 mV). The tip of the electrode was 4–8 MΩ when filled with patch pipette internal solution containing (in mmol/L): 120 $CsMeSO_3$, 2 NaCl, 20 HEPES, 5 tetraethylammonium-Cl, 2.5 Na_2ATP, 0.4 EGTA 0.3 GTP-Tris, and 2.5 mmol/L QX-314 (pH 7.2–7.4, adjusted with CsOH). A concentric bipolar electrode was placed at the border between the prefrontal cortex (PFC) and NAc, which mainly stimulated the PFC-synaptic transmission input to the MSNs [23]. Synaptic afferents were stimulated at 0.1 Hz (100-μs pulses) by a programmable stimulator (Master-8, A.M.P.I., Jerusalem, Israel). The stimulation intensity that evoked a half-maximum synaptic response was used in the experiments. Input resistance was monitored online with a depolarizing step voltage (+ 5 mV, 200 ms) following each afferent stimulus, and the data were discarded if the resistance changed by $> 25\%$. Total evoked postsynaptic currents of NAc shell MSNs containing AMPAR-mediated EPSCs and $GABA_A$-receptor-mediated IPSCs were recorded at a holding voltage of – 70 mV in normal aCSF. After recording a stable total postsynaptic current baseline, the AMPAR-mediated EPSC was isolated by perfusing with the $GABA_A$ receptor antagonist picrotoxin (PTX, 100 μmol/L), and digital subtraction of the AMPAR-mediated EPSC from the total postsynaptic current in the same neuron yielded the $GABA_A$-receptor-mediated IPSC. For sEPSC recording, the membrane voltage was held at – 70 mV and the cells were perfused by aCSF with 100 μmol/L PTX and 1 μmol/L strychnine. The sIPSCs were recorded with the voltage held at 0 mV (because the reversal potential for EPSCs was near 0 mV), and 1 μmol/L strychnine was added to the aCSF to block glycine receptor-mediated IPSCs. To calculate ratios of sEPSC/sIPSC peak amplitude and frequency, the sIPSCs and sEPSCs were recorded from the same neuron. Traces for the analyzed ratios were averaged from 80–100 consecutive sIPSCs or sEPSCs. To determine the paired-pulse ratio (PPR), which reflects the transmitter release probability at presynaptic sites, two IPSCs or EPSCs were evoked at an inter-stimulus-interval of 50 ms or 200 ms. The PPR value was calculated by dividing the amplitude of the second event by that of the first event. LTD was induced by low-frequency stimulation (LFS, pulse duration 100 μs, 1 Hz, 900 pulses). The stimulating electrode was positioned at the same location as that in the evoked EPSCs and IPSCs recording.

The total spontaneous miniature EPSCs (mEPSCs) that contain both NMDAR- and AMPAR-mediated components were recorded in the presence of tetrodotoxin (1 μmol/L) and PTX (100 μmol/L) and patch-clamped at –60 mV with Mg^{2+}-free aCSF perfusion. The AMPAR- and NMDAR-mediated mEPSCs were isolated by perfusing with the NMDAR antagonist AP–V (50 μmol/L). AMPAR- and NMDAR-mEPSC components were analyzed as previously described [23]. NMDA-induced currents were recorded by puff application of NMDA (20 μmol/L; Sigma-Aldrich) at a holding potential of –45 mV.

Data Analysis and Statistics

Results are expressed as the mean ± SEM. Each data set to be tested statistically was first tested for normality by the Shapiro-Wilk test. If data were not normally distributed, we used the non-parametric Mann-Whitney test. Otherwise, the data were analyzed *via* Student's *t*-test, one-way or two-way ANOVA with repeated-measures (RM) or regular ANOVA measures, followed by the LSD *post hoc* test. The inter-event intervals and amplitudes for the distribution of sIPSCs or sEPSCs were measured with Kolmogorov–Smirnov (K–S) analysis and the unpaired Student's *t*-test. The criterion of statistical significance was set at $P < 0.05$.

Results

SNL Decreases the E/I Ratio in MSNs of the NAc Shell

Our previous study has shown that SNL induces persistent pain hypersensitivity and depression-like behaviors [3]. To understand the synaptic mechanism underlying the behavioral changes after SNL, we performed whole-cell patch-

clamp recordings of EPSCs and IPSCs from the same MSNs in the NAc shell. The stimulating electrode was positioned at the border of the PFC and NAc within the brain slice to elicit a compound postsynaptic current, which contains both EPSCs and IPSCs. After recording a stable total current, we perfused the slice with PTX to selectively inhibit IPSCs, then subtracted the PTX-insensitive current to get the IPSC component (Fig. 1A). We found that the EPSC/IPSC ratio was markedly reduced in mice with SNL ($P < 0.01$, Student's t-test, Fig. 1B, C). To identify the effect of SNL on the strength of the excitatory and inhibitory synaptic transmission, we examined the input-output (I–O) curves from the glutamatergic and the GABAergic synapse-mediated currents. Compared with the sham group, SNL significantly suppressed the amplitude of the evoked EPSCs ($F_{1,30} = 8.065$, $P < 0.01$, two-way ANOVA with repeated-measures, Fig. 1D), and markedly increased the amplitude of the evoked IPSCs in MSNs ($F_{1,20} = 8.179$, $P < 0.05$, two-way ANOVA with repeated-measures, Fig. 1E). These data suggest that the E/I balance in MSNs of the NAc shell is disrupted after SNL.

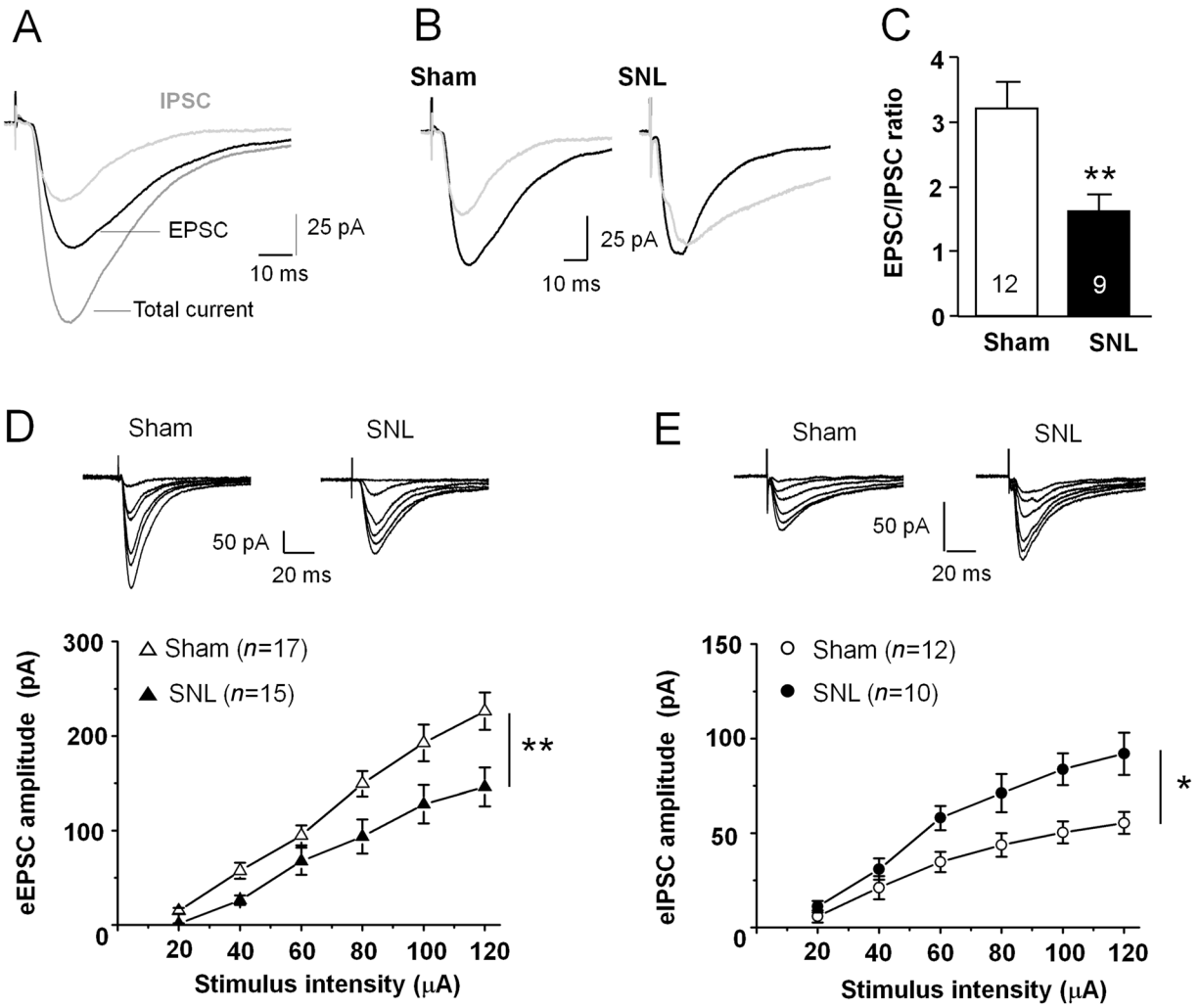

Fig. 1 SNL disrupts the excitatory/inhibitory (E/I) balance at MSN synapses in the NAc shell. **A** Sample traces showing total current, an EPSC, and an IPSC in the same MSN. **B** Sample traces showing EPSCs (black traces) and IPSCs (grey traces) in the same MSN from sham- and SNL-operated mice. **C** The mean EPSC/IPSC ratio is decreased in SNL-operated mice (**$P < 0.01$, Student's t-test). **D** Upper panel, sample traces of EPSCs evoked by stimulation intensity from 20 μA to 120 μA. Each trace is averaged from 6–10 EPSCs at the same stimulus intensity. Lower panel, summary data showing that SNL decreases the input–output response of eEPSCs (15–17 neurons from 4–5 mice, **$P < 0.01$, two-way ANOVA with repeated-measures). **E** Upper panel, sample traces of GABAergic receptor-mediated IPSCs evoked by stimulation intensity from 20 μA to 120 μA from sham- and SNL-operated mice. Each trace is averaged from 6–10 IPSCs at the same stimulus intensity. SNL increases the input–output response of eIPSCs in NAc shell MSNs (10–12 neurons from 4–5 mice, *$P < 0.05$, two-way ANOVA with repeated-measures). Both EPSCs and IPSCs are shown at the peak of the current responses.

SNL Increases Inhibitory Synaptic Transmission in MSNs

To study the detailed changes of inhibitory and excitatory synaptic transmission in MSNs of the NAc shell after SNL, we first examined the inhibitory synaptic component. The sIPSCs were recorded in MSNs from the sham- or SNL-operated mice by holding the membrane potential at 0 mV (Fig. 2A). We analyzed the cumulative probability distributions of inter-event intervals of sIPSCs and found that the cumulative fraction was significantly shifted to the left in SNL mice compared with sham-operated mice ($P < 0.01$, K–S test, Fig. 2B). The mean frequency of sIPSCs was significantly increased in SNL animals ($P < 0.01$, Mann-Whitney test, Fig. 2C). There was no significant difference in the amplitude of sIPSCs between sham and SNL-operated mice ($P > 0.05$, Mann-Whitney test, Fig. 2D, E).

SNL Decreases Excitatory Synaptic Transmission in MSNs

To determine whether the disrupted balance was affected by excitatory synaptic transmission in SNL animals, we directly measured the sEPSCs by holding the membrane potential at – 70 mV in MSNs of NAc slices from sham- or SNL-operated mice in the presence of PTX (100 μmol/L) and strychnine (1 μmol/L) to exclude $GABA_A$ receptor- and glycine receptor-mediated inhibitory synaptic inputs (Fig. 3A). The cumulative probability distribution of inter-event intervals of sEPSCs shifted to the right after SNL ($P < 0.01$, K–S test, Fig. 3B). The mean frequency of

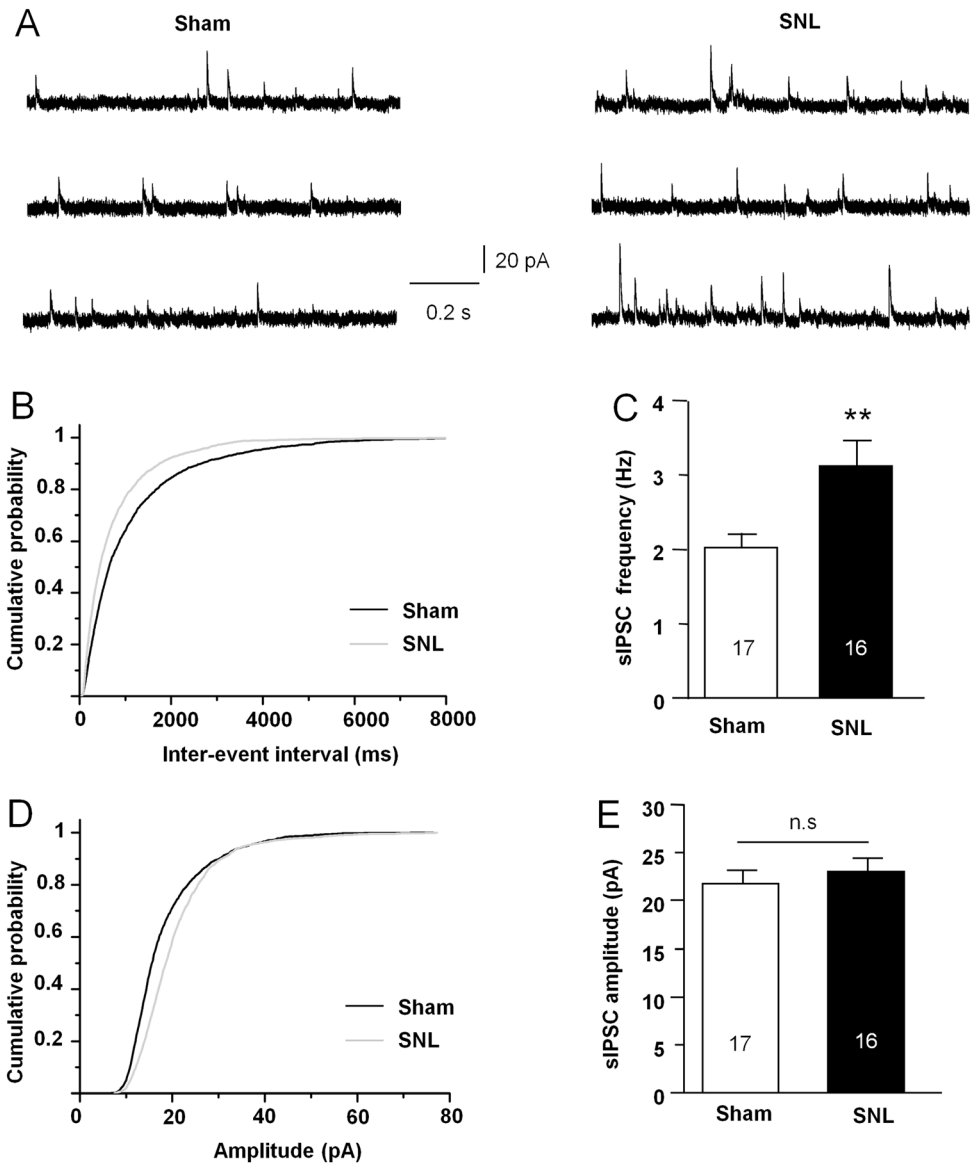

Fig. 2 SNL enhances the sIPSC frequency in MSNs in the NAc shell. **A** Sample traces of sIPSCs recorded from MSNs in sham- and SNL-operated mice. **B** Cumulative probability distribution of sIPSC inter-event intervals is shifted to the left after SNL ($P < 0.01$, K–S test). **C** The mean sIPSCs frequency is increased in MSNs after SNL (**$P < 0.01$, Mann-Whitney test). **D** Cumulative probability distribution for sIPSC amplitude is not significantly different in sham- and SNL-operated animals ($P > 0.05$, K–S test). **E** The mean sIPSC amplitude is comparable in the two groups ($P > 0.05$, n.s., not significant, Mann-Whitney test).

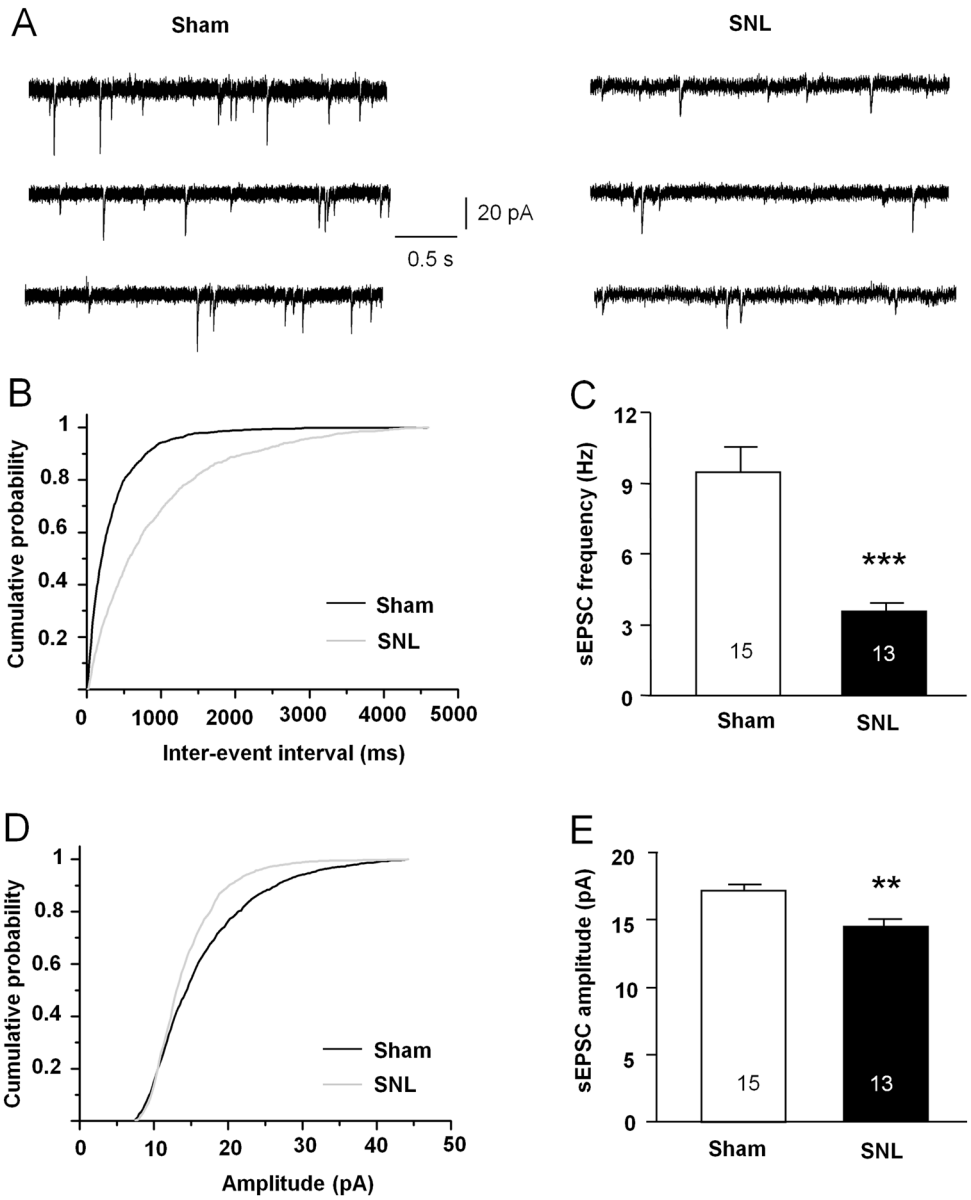

Fig. 3 SNL suppresses the sEPSC frequency and amplitude in MSNs in the NAc shell. **A** Sample traces of sEPSCs recorded from NAc shell MSNs in sham- and SNL-operated mice. **B** Cumulative probability distribution of sEPSC inter-event intervals is shifted to the right after SNL ($P < 0.01$, K–S test). **C** The mean sEPSC frequency is decreased in MSNs after SNL (***$P < 0.001$, Student's *t*-test). **D** Cumulative probability distribution for sEPSC amplitude in MSNs from SNL-operated mice is shifted to the left relative to the sham-treated group ($P < 0.01$, K–S test). E Mean sEPSC amplitude is decreased in MSNs after SNL (**$P < 0.01$, Mann-Whitney test).

sEPSCs was significantly decreased in SNL-operated animals ($P < 0.001$, Student's *t*-test, Fig. 3C). The distribution of sEPSCs amplitudes shifted to the left after SNL ($P < 0.05$, K–S test, Fig. 3D). The mean amplitude of sEPSCs was decreased in SNL-operated animals ($P < 0.01$, Mann-Whitney test, Fig. 3E).

SNL Leads to Different Changes in the PPR of eIPSCs and eEPSCs in MSNs

To further determine the change of presynaptic GABA and glutamate release, we compared the paired-pulse ratio (PPR) in NAc slices from sham- and SNL-operated mice. The PPR of eIPSCs was elicited by two pulses at 50-ms or 200-ms inter-pulse intervals in the presence of the AMPAR antagonist DNQX and the NMDAR antagonist AP-V. The PPR of eIPSCs was significantly lower in SNL mice than in sham-operated mice with the 50-ms inter-pulse interval, but no such change was found with the 200-ms inter-pulse interval (50 ms, $P < 0.01$; 200 ms, $P > 0.05$. Student's *t*-test, Fig. 4A, B). The same was found in the eEPSC PPR, which was elicited in the presence of the $GABA_A$ receptor antagonist PTX and the glycine receptor antagonist strychnine. In contrast, the PPR of eEPSCs was significantly higher in the SNL group than in the sham group at the 50-ms inter-pulse interval; no difference was found at the 200-ms inter-pulse interval (50 ms, $P < 0.01$; 200 ms, $P > 0.05$, Student's *t*-test, Fig. 4C, D).

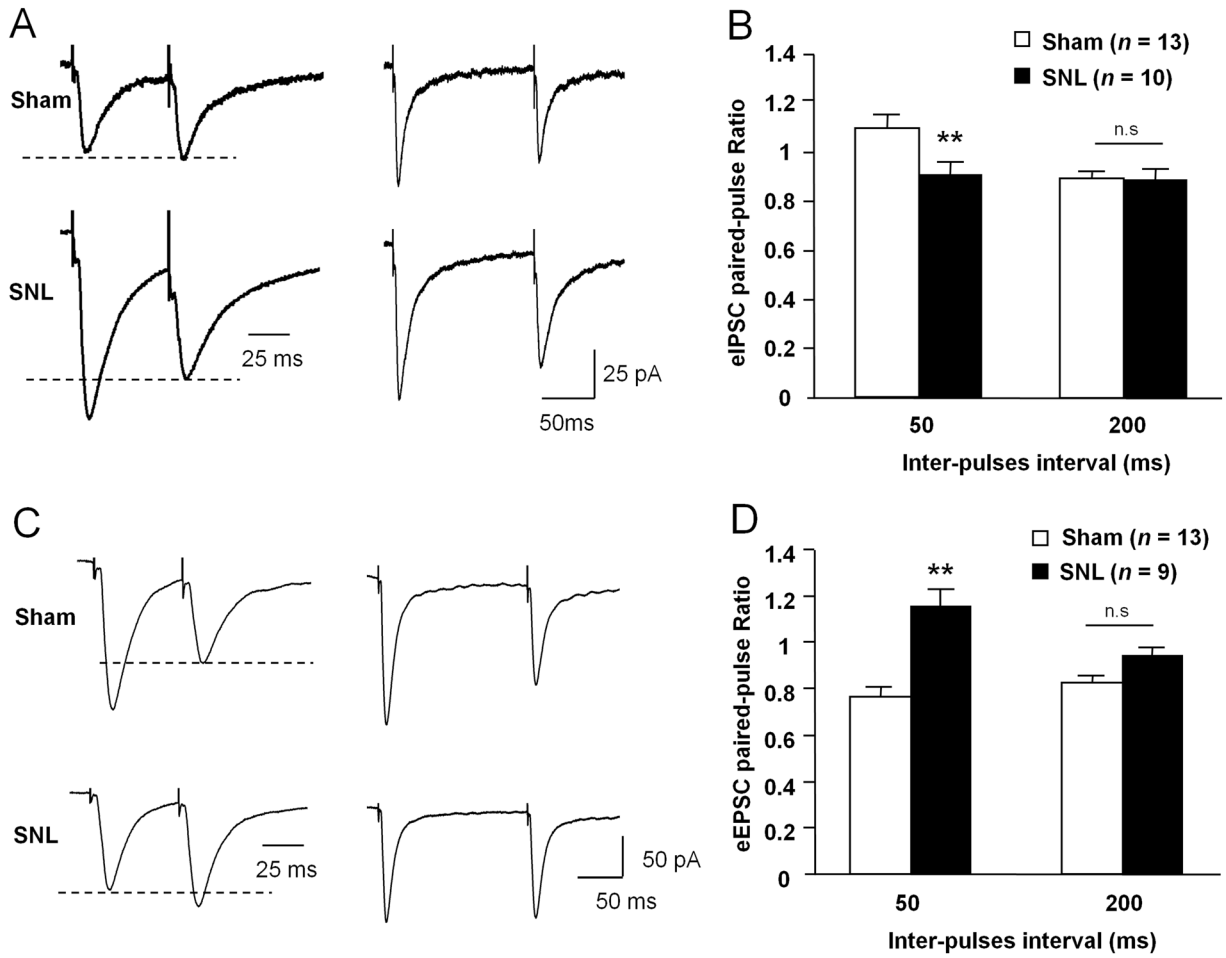

Fig. 4 SNL differentially changes the PPR of eIPSCs and eEPSCs in MSNs in the NAc shell. **A** Sample traces of IPSCs evoked by paired-pulse stimulation with inter-pulse intervals of 50 ms (left) and 200 ms (right) in MSNs from sham- and SNL-operated mice. **B** The mean PPR of eIPSCs is decreased after SNL at inter-pulse intervals of 50 ms (**$P < 0.01$, Student's *t*-test), but not at inter-pulse intervals of 200 ms. **C** Sample traces of EPSCs evoked by paired-pulse stimulation with inter-pulse intervals of 50 ms (left) and 200 ms (right) in MSNs from sham- and SNL-operated mice. **D** The mean PPR of eEPSCs is increased after SNL at inter-pulse intervals of 50 ms (** $P < 0.01$, n.s., not significant, Student's *t*-test), but not at 200 ms.

CCL2/CCR2 Signaling Regulates Inhibitory and Excitatory Synaptic Inputs in MSNs of the NAc Shell

To explore the molecular mechanisms underlying the disruption of E/I balance after SNL, we tested the role of CCL2/CCR2 in synaptic transmission in MSNs, as CCL2 and CCR2 are markedly increased in the NAc shell after SNL [3]. We first determined whether CCL2 affects inhibitory GABAergic synaptic transmission and found that the frequency and amplitude of sIPSCs were significantly increased by acute CCL2 perfusion compared with baseline (frequency, 149.9% ± 13.7%, $P < 0.05$; amplitude, 134.5% ± 9.9%, $P < 0.05$, paired Student's *t*-test, Fig. 5A and B). Similarly, bath application of CCL2 also increased the frequency and amplitude of sEPSCs (frequency, 144.3% ± 8.1%, $P < 0.001$; amplitude, 110.5% ± 4.2%, $P < 0.05$, paired Student's *t*-test, Fig. 5C, D). As SNL persistently increased CCL2 expression in the NAc shell [3], we further investigated how chronic activation of CCL2/CCR2 signaling regulates E/I input to NAc shell MSNs. The *Ccl2*-overexpressing lentivirus (LV-*Ccl2*) or LV-*NC* was microinjected into the NAc shell. Ten days later, we recorded the sEPSCs and sIPSCs from the same MSN, and then calculated their mean peak amplitudes. Compared with the LV-*NC*-treated mice, LV-*Ccl2* moderately weakened the sEPSC/sIPSC frequency ratio and significantly decreased the peak amplitude ratio in NAc shell MSNs ($P < 0.05$, Student's *t*-test, Fig. 5G), similar to the results from SNL-operated mice.

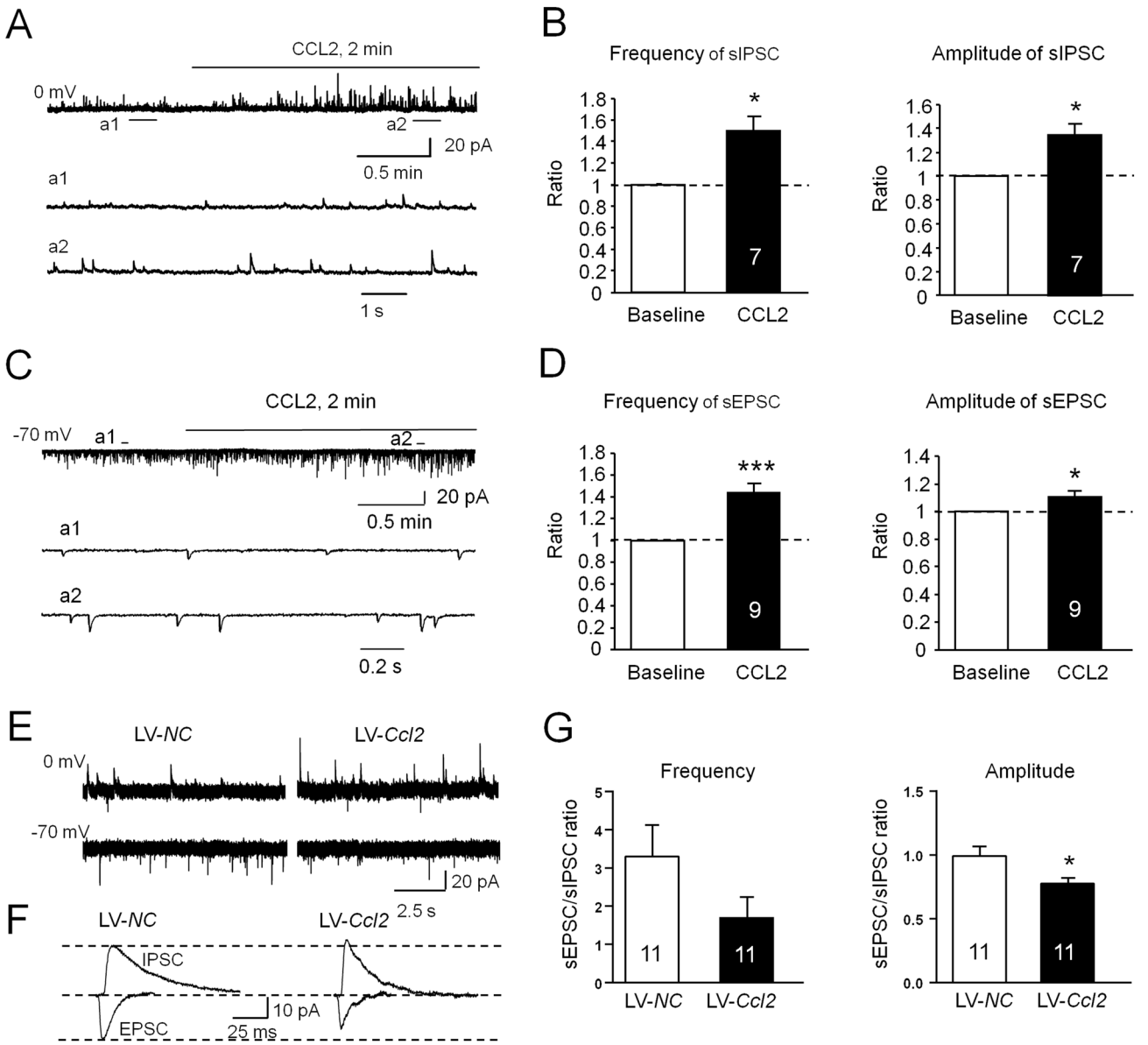

Fig. 5 Effects of CCR2 activation on the sIPSC/sEPSC ratio in MSNs in the NAc shell. **A** Sample traces of sIPSCs from NAc shell MSNs in naive mice after CCL2 (100 nmol/L) application. **a1**, **a2** Expanded traces of sIPSCs recorded in the absence (**a1**) and presence (**a2**) of CCL2. **B** sIPSC frequency and amplitude is increased by CCL2 application (*$P < 0.05$, paired Student's *t*-test). **C** Sample traces of sEPSCs from NAc shell MSNs in naive mice after CCL2 (100 nmol/L) bath application. **a1**, **a2** Expanded sEPSC traces recorded in the absence (**a1**) and presence (**a2**) of CCL2. **D** sEPSC frequency and amplitude are increased by CCL2 application (*$P < 0.05$, ***$P < 0.001$, paired Student's *t*-test). **E** Sample traces of sIPSCs (held at 0 mV) and sEPSCs (held at – 70 mV) from the same MSN in naïve mice pretreated with LV-*NC* or LV-*Ccl2*. **F** Representative averaged traces of sIPSCs and sEPSCs from NAc shell MSNs (data from **E**). **G** Histograms of ratios of EPSC/IPSC frequency and amplitude from mice pretreated with LV-*NC* or LV-*Ccl2*. (LV-*NC* *vs* LV-*Ccl2*: frequency: $P > 0.05$; amplitude: *$P < 0.05$, Student's *t*-test)

Acute CCR2 Activation Strengthens NMDAR Function in MSNs

Our previous study showed that SNL increases the NMDAR currents in MSNs, and that they are reduced by *Ccr2* shRNA or a CCR2 antagonist [3]. We further assessed the effect of acute activation of CCR2 by CCL2 on NMDAR-mediated EPSCs in the MSNs. The amplitudes of NMDAR- and AMPAR-mEPSCs were compared in the presence or absence of CCL2 (Fig. 6A, B). The amplitude of NMDAR-mEPSCs was larger in CCL2-incubated neurons than that in vehicle control ($P < 0.05$, paired Student's *t*-test, Fig. 6C), but no statistical difference was found in the mean amplitude of AMPAR-mEPSCs between the two conditions ($P > 0.05$, paired Student's *t*-test, Fig. 6C). In addition, the amplitude

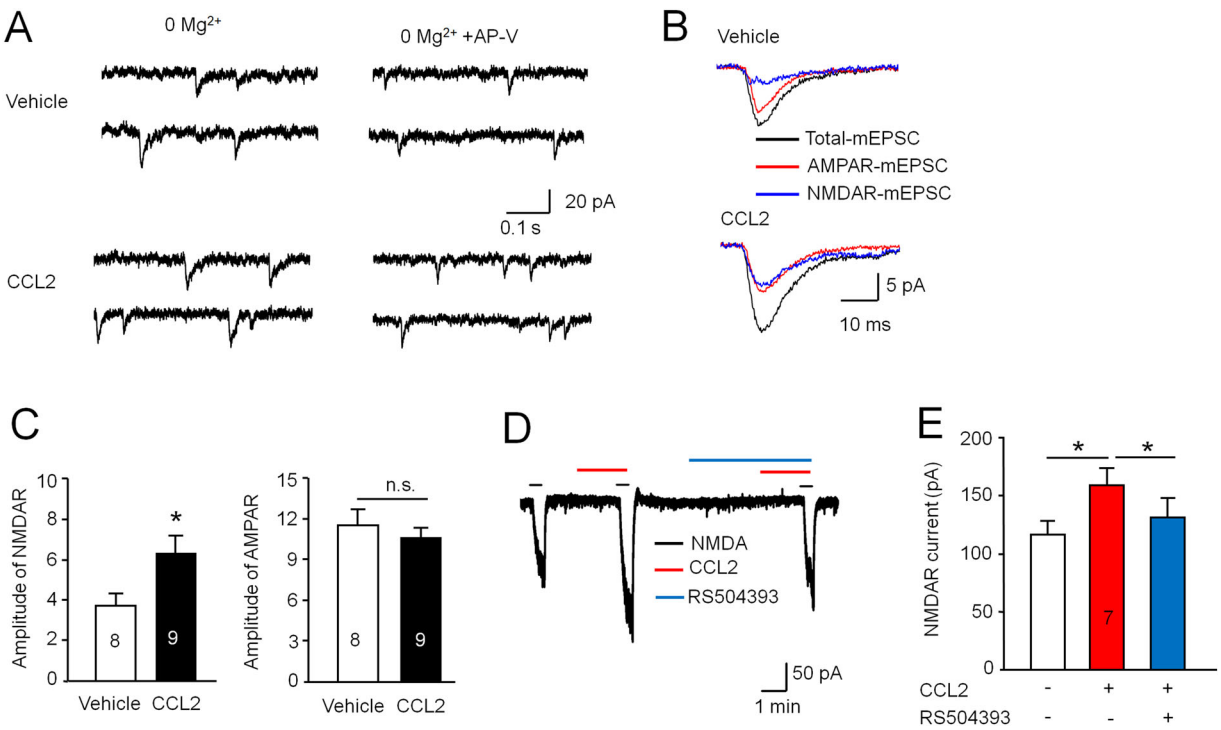

Fig. 6 Activation of CCL2/CCR2 signaling strengthens NMDAR-mediated EPSCs in NAc shell MSNs. **A** Sample traces of mEPSCs from NAc shell MSNs patch-clamped at –60 mV in Mg^{2+}-free aCSF. Total mEPSCs (left) include both NMDAR- and AMPAR-mediated components. AMPAR-mediated mEPSCs (right) were isolated by perfusing with the NMDAR antagonist AP-V (50 μmol/L) in the absence and presence of CCL2. **B** Average traces of total mEPSCs, AMPAR-mEPSCs, and NMDAR-mEPSCs from MSNs in the absence and presence of CCL2. **C** Histograms of AMPAR- and NMDAR-mEPSC amplitude in the absence (vehicle) and presence of CCL2 in aCSF (*$P < 0.05$, Student's *t*-test). **D** Sample trace of NMDA (20 μmol/L, 30 s)-induced current recorded in Mg^{2+}-free aCSF solution; this is enhanced in the presence of CCL2 and prevented by RS504393 (10 μmol/L), a selective antagonist of CCR2. **E** Histograms of the amplitude of NMDA-induced currents with or without CCL2 incubation and pre-incubation with RS504393 in the aCSF (*$P < 0.05$, paired Student's *t*-test).

of inward current evoked by 20 μmol/L NMDA was markedly increased by CCL2 application, and this effect was prevented by the CCR2 antagonist RS504393 ($P < 0.05$, paired Student's *t*-test, Fig. 6D, E). These data suggest that CCL2/CCR2 contributes to the imbalance of inhibitory and excitatory synaptic transmission on MSNs *via* regulating NMDAR function after SNL.

CCR2 Knock-down Improves the Impaired NMDAR-dependent LTD Induction in the NAc Shell after SNL

To determine whether LTD occurs *in vivo* at MSN glutamatergic synapses after SNL, we used LFS (1 Hz, 900 pulses) to evoke LTD in NAc slices. Robust LTD was evoked (45.8% ± 4.8% of baseline, $P < 0.001$ *vs* baseline, Student's *t*-test) at MSN synapses in the naive mice. This LTD was attenuated by the GluN2B-containing NMDAR-selective antagonist Ro 25-6981 (85.2% ± 7.3% of baseline), but was unaffected by the GluN2A-containing NMDAR-selective antagonist TCN-201 (55.5% ± 10.3% of baseline, $P < 0.05$ *vs* baseline, Student's *t*-test). The magnitude of LTD was different in the control and Ro 25-6981-treated groups ($F_{2,19} = 9.66$, $P < 0.01$, one-way ANOVA followed by LSD test, Fig. 7A, B). We then examined the LTD induction in the sham and SNL-operated groups. The magnitude of LTD was lower in the SNL group (73.3% ± 6.4 % of baseline, $P < 0.01$ *vs* baseline, Student's *t*-test) than that in the sham group (47.9% ± 3.2% of baseline, $P < 0.001$ *vs* baseline; Sham *vs* SNL, $P < 0.01$, Student's *t*-test, Fig. 7C, D). To determine whether CCR2 in the NAc was involved in the impairment of NMDAR-dependent LTD induction after SNL, we injected *Ccr2* shRNA lentivirus (LV-*Ccr2* shRNA) into the NAc shell 7 days before SNL. Compared with control lentivirus treatment, LV-*Ccr2* shRNA prevented the decrease in the magnitude of NMDAR-dependent LTD induction after SNL (LV-*NC*-SNL: 79.9% ± 8.9% of baseline; LV-*Ccr2*-SNL: 59.8% ± 4.1% of baseline, $P < 0.01$ *vs* baseline, LV-*NC* *vs* LV-*Ccr2*-SNL, $P = 0.06$, Student's *t*-test, Fig. 7E, F). These results indicate that the reduction of the magnitude of NMDAR-dependent LTD in the NAc was rescued by the knock-down of *Ccr2* in SNL animals.

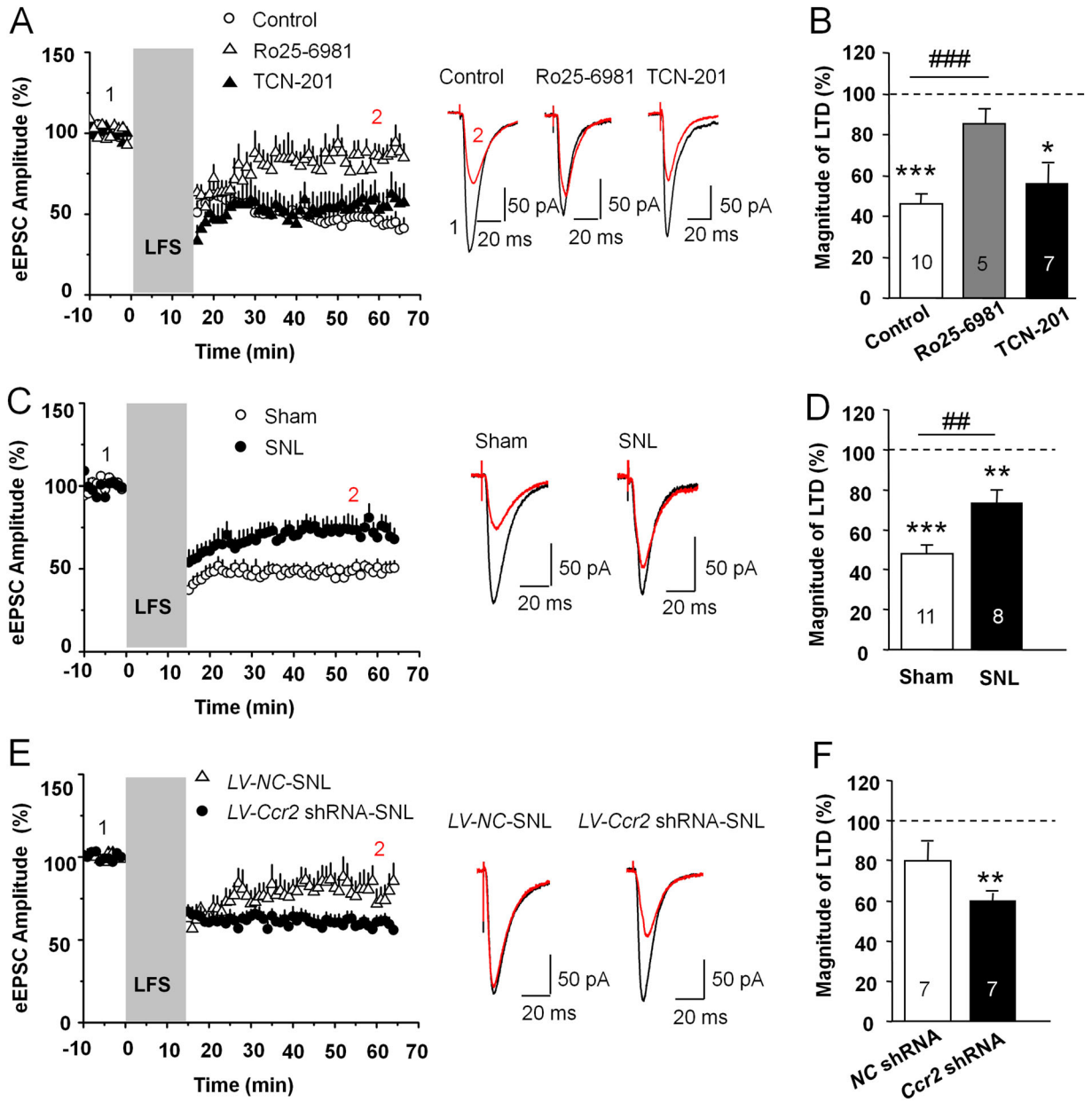

Fig. 7 CCR2 knock-down improves the attenuated NMDAR-dependent LTD in MSNs of the NAc shell after SNL. **A** Left panel, normalized values of evoked EPSCs amplitude showing long-term synaptic plasticity [grey band, LFS duration (1 Hz; 900 pulses)]. LFS decreases eEPSC amplitude in the NAc shell under control condition. LTD induction is impaired by Ro 25-6981 (3 μmol/L), but is not changed by TCN-201 (1 μmol/L). Right panel, sample eEPSCs before and 30 min after LTD induction in control and Ro 25-6981- or TCN-201-treated slices. **B** Normalized mean magnitude of LTD measured 30 min after LFS stimulation in control, Ro 25-6981-perfused, or TCN-201-perfused slices (*$P < 0.05$, ***$P < 0.001$, *vs* baseline, Student's *t*-test. ### $P < 0.001$, *vs* control, one-way ANOVA followed by LSD test). **C** Left panel, LFS induced-LTD is reduced in SNL-operated mice. Right panel, sample eEPSCs before and 30 min after LTD induction in sham- and SNL-operated mice. **D** Normalized mean magnitude of LTD measured 30 min after LFS stimulation in sham and SNL mice (**$P < 0.01$, *** $P < 0.001$, *vs* baseline. ## $P < 0.01$, *vs*. sham. Student's *t*-test). **E** SNL leads to impaired NMDAR-LTD in LV-*NC*-injected mice, and this is rescued by LV-*Ccr2*-shRNA injection. Right panel, sample traces before and 30 min after LTD induction in SNL mice. **F** Normalized mean magnitude of LTD measured 30 min after LFS stimulation in LV-*NC* or LV-*Ccr2*-shRNA injected mice (**$P < 0.01$, *vs* baseline. Student's *t*-test).

Discussion

In the current study, we for the first time showed that CCL2/CCR2 contributed to the altered excitatory and inhibitory balance in the MSNs of NAc shell. The NAc plays a crucial role in the transition from acute to chronic pain [24, 25], and is involved in the affective component during a chronic pain state [15]. As an important area in pain regulation, the output dynamics of the NAc depends on the intrinsic neuronal excitability and overall balance of excitatory and inhibitory synaptic inputs. Recent work has indicated that peripheral nerve injury increases the intrinsic excitability of NAc shell MSNs [2]. Furthermore, inactivating these cells reverses the pain sensitivity, and exciting these cells exacerbates tactile allodynia [2]. Blocking NMDARs in the NAc alleviates nociceptive behaviors and the related affect [3]. Here we found that the EPSC/IPSC ratio was decreased in the SNL-induced neuropathic pain model, and this was partly caused by reduced excitatory synaptic strength. Consistent with this, a previous study showed that the AMPAR/NMDAR current ratio, which reflects basal synaptic transmission strength [23], is decreased in the NAc MSNs of mice with spinal nerve injury [1]. NAc neurons mainly receive excitatory glutamatergic synaptic inputs from the PFC, ventral hippocampus, and basal lateral amygdala [26], and integrate inhibitory GABAergic synaptic inputs from local neurons and the PFC [27, 28]. Spinal nerve injury strengthens the AMPAR/NMDAR current ratio at ventral hippocampus-NAc synapses in dopamine D2 receptor-positive MSNs, but decreases this ratio at PFC-NAc synapses in these MSNs [2]. Similarly, we found a significant reduction in the I-O curves of PFC-NAc excitatory glutamatergic synaptic inputs after SNL. In addition, the reduced EPSC/IPSC ratio may also be caused by increased inhibitory synaptic strength. We also found that SNL increased the I-O curves of inhibitory GABAergic synaptic inputs to the MSNs. In the NAc, synaptic inhibition is mainly mediated by local GABAergic interneurons, which also express parvalbumin or somatostatin [29]. MSNs, as GABAergic projection neurons, can regulate local circuitry by lateral inhibition [28, 29]. Thus, the origin of the changed synaptic inputs to MSNs needs further study.

Our data also showed that the frequency of sIPSCs in NAc MSNs was significantly increased, while the sIPSCs amplitude was not changed, suggesting enhanced presynaptic GABAergic transmitter release at the synapses of NAc MSNs after SNL. Scaling of GABAergic transmission can be triggered by postsynaptic NMDAR-mediated calcium increase, which subsequently enhances GABA release through retrograde activation of the presynaptic NMDARs of interneurons [30]. It has been reported that brain-derived neurotrophic factor (BDNF) increases inhibitory GABAergic synaptic efficacy in the hippocampus and cortex [31, 32]. BDNF is increased in the NAc during neuropathic pain [33, 34]. Thus, BDNF in the NAc might play a role in regulating inhibitory GABAergic synaptic efficacy on MSNs through presynaptic TrkB signaling in the GABAergic interneurons [35, 36]. In contrast to the inhibitory synapse, we found a reduction of excitatory synaptic inputs which may be caused by decreased presynaptic glutamate release or a decrease in the activity of postsynaptic glutamatergic receptors after SNL. It has been reported that the decreased postsynaptic AMPAR-mediated currents after SNL may contribute to the attenuation of glutamatergic synaptic transmission in neuropathic pain [1, 2]. SNL also led to differential changes in the PPR of eIPSCs and eEPSCs, further indicating that a presynaptic mechanism plays a role in the disruption of E/I balance in NAc MSNs, which may contribute to neuropathic pain and depression.

Our recent study showed that the expression of CCL2 and CCR2 are persistently increased in the NAc shell after SNL, and CCL2/CCR2 signaling is involved in the regulation of SNL-induced neuropathic pain and depressive-like behaviors [3]. Bath application of CCL2 increased the frequency and amplitude of sIPSCs in NAc shell MSNs, suggesting that CCL2/CCR2 signaling increases the presynaptic transmitter release from GABAergic synapses and increases the activity of $GABA_A$ receptors. However, previous studies have reported that the frequency, not the amplitude of sEPSCs is increased in dorsal horn neurons [37] and hippocampus neurons [17] after CCR2 activation, suggesting that CCL2/CCR2 signaling has a presynaptic site of action in the spinal cord and hippocampus. We also found that bath application of CCL2 caused an increase of sEPSCs, suggesting that acute activation of CCR2 potentially leads to transient homeostatic synaptic plasticity to maintain the balance of excitatory and inhibitory inputs to the MSNs [38]. In contrast, persistent activation of CCR2 by LV-*Ccl2* decreased the E/I ratio in the MSNs in the NAc, similar to the changes after SNL, suggesting that persistent CCL2/CCR2 upregulation contributes to resetting of E/I ratio under chronic pain conditions. It has been reported that resetting the E/I balance may increase NMDAR activation and further regulate the long-term form of glutamatergic synaptic plasticity [38]. Indeed, SNL-induced CCR2 activation amplifies the NMDAR-mediated currents in NAc MSNs [3]. We found that the amplitude of NMDAR-mEPSCs, but not of AMPAR-mEPSCs was increased after CCR2 activation. Direct perfusion of the NAc slice with CCL2 increased the NMDA-induced inward current in MSNs, and this was suppressed in the presence of the CCR2 antagonist RS504393. Similarly, bath application of CCL2 enhances

both NR2A- and NR2B-subunit-containing NMDAR EPSCs in hippocampal neurons [17]. Moreover, overexpression of CCL2 by intra-NAc injection of *Ccl2*-expressing lentivirus increased the protein level of phosphorylated NR2B *via* the mitogen-activated protein kinase signaling pathway in the NAc [3]. Overall, these results suggest that CCR2 may regulate the strength of synaptic transmission *via* both presynaptic and postsynaptic effects in the NAc.

Abnormalities of excitatory synaptic function in chronic pain include changes in the frequency and amplitude of sEPSC and the input-output of evoked EPSCs, as well as impairments in the threshold for LTD/LTP induction [39]. Here, LTD was induced at synapses of NAc MSNs with LFS [40, 41]; it was blocked by the selective GluN2B antagonist Ro 25-6981, but was not affected by the GluN2A-containing NMDAR antagonist TCN-201. The enhancement of GluN2B-containing NMDAR at postsynaptic sites might be required for the synaptic depression [42]. Recent investigation indicated that spinal nerve injury induces a significant increase in NMDAR-mediated currents, and impairs LFS-induced LTD at synapses on NAc dopamine D2-positive MSNs [1]. Here, knockdown of *Ccr2* rescued the impaired LTD induction after SNL. In addition, knockdown of *Ccr2* expression in the NAc relieved SNL-induced neuropathic pain and depression *via* suppressing NMDAR function [3]. Thus, CCL2 and CCR2 may contribute to the disruption of E/I input to the MSNs, which further caused the damage of LTD induction in SNL. The forms of synaptic transmission abnormalities may be different in different brain regions and cell types, or under different experiment conditions, and these abnormalities may contribute to the sensory and affective behavior adaptations during chronic pain [43, 44].

In summary, the current study showed that SNL disrupted the E-I balance at the synapses of NAc shell MSNs. This maladaptation was related to changes in both excitatory glutamatergic synaptic transmission and inhibitory GABAergic inhibitory synaptic transmission. The enhancement of inhibitory synaptic inputs may be due to an increase of presynaptic GABAergic transmitter and the suppression of excitatory glutamatergic synaptic inputs. CCL2/CCR2 signaling may contribute to the excitatory and inhibitory synaptic adaptations which potentially modulate LTD induction at the synapses of NAc MSNs during chronic pain.

Acknowledgements This work was supported by Grants from the National Natural Science Foundation of China (32030048, 31871064, and 31671091).

Conflict of interest The authors declare that they have no conflict of interest.

References

1. Schwartz N, Temkin P, Jurado S, Lim BK, Heifets BD, Polepalli JS, *et al.* Chronic pain. Decreased motivation during chronic pain requires long-term depression in the nucleus accumbens. Science 2014, 345: 535–542.
2. Ren W, Centeno MV, Berger S, Wu Y, Na X, Liu X. The indirect pathway of the nucleus accumbens shell amplifies neuropathic pain. Nat Neurosci 2016, 19: 220–222.
3. Wu XB, Jing PB, Zhang ZJ, Cao DL, Gao MH, Jiang BC, *et al.* Chemokine receptor CCR2 contributes to neuropathic pain and the associated depression *via* increasing NR2B-mediated currents in both D1 and D2 dopamine receptor-containing medium spiny neurons in the nucleus accumbens shell. Neuropsychopharmacology 2018, 43: 2320–2330.
4. Chang PC, Pollema-Mays SL, Centeno MV, Procissi D, Contini M, Baria AT, *et al.* Role of nucleus accumbens in neuropathic pain: linked multi-scale evidence in the rat transitioning to neuropathic pain. Pain 2014, 155: 1128–1139.
5. Goffer Y, Xu D, Eberle SE, D'Amour J, Lee M, Tukey D, *et al.* Calcium-permeable AMPA receptors in the nucleus accumbens regulate depression-like behaviors in the chronic neuropathic pain state. J Neurosci 2013, 33: 19034–19044.
6. Xu D, Su C, Lin HY, Manders T, Wang J. Persistent neuropathic pain increases synaptic GluA1 subunit levels in core and shell subregions of the nucleus accumbens. Neurosci Lett 2015, 609: 176–181.
7. Su C, D'Amour J, Lee M, Lin HY, Manders T, Xu D, *et al.* Persistent pain alters AMPA receptor subunit levels in the nucleus accumbens. Mol Brain 2015, 8: 46.
8. Nisenbaum ES, Grace AA, Berger TW. Functionally distinct subpopulations of striatal neurons are differentially regulated by GABAergic and dopaminergic inputs–II. vitro analysis. Neuroscience 1992, 48: 579–593.
9. Russo SJ, Mazei-Robison MS, Ables JL, Nestler EJ. Neurotrophic factors and structural plasticity in addiction. Neuropharmacology 2009, 56(Suppl 1): 73–82.
10. Wilson CJ, Kawaguchi Y. The origins of two-state spontaneous membrane potential fluctuations of neostriatal spiny neurons. J Neurosci 1996, 16: 2397–2410.
11. O'Donnell P, Grace AA. Synaptic interactions among excitatory afferents to nucleus accumbens neurons: hippocampal gating of prefrontal cortical input. J Neurosci 1995, 15: 3622–3639.
12. Castillo PE, Chiu CQ, Carroll RC. Long-term plasticity at inhibitory synapses. Curr Opin Neurobiol 2011, 21: 328–338.
13. Potter LE, Paylor JW, Suh JS, Tenorio G, Caliaperumal J, Colbourne F, *et al.* Altered excitatory-inhibitory balance within somatosensory cortex is associated with enhanced plasticity and pain sensitivity in a mouse model of multiple sclerosis. J Neuroinflammation 2016, 13: 142.
14. Cheriyan J, Sheets PL. Peripheral nerve injury reduces the excitation-inhibition balance of basolateral amygdala inputs to prelimbic pyramidal neurons projecting to the periaqueductal gray. Mol Brain 2020, 13: 100.
15. Massaly N, Copits BA, Wilson-Poe AR, Hipolito L, Markovic T, Yoon HJ, *et al.* Pain-induced negative affect is mediated *via* recruitment of the nucleus accumbens kappa opioid system. Neuron 2019, 102(564–573): e566.
16. Gao YJ, Zhang L, Samad OA, Suter MR, Yasuhiko K, Xu ZZ, *et al.* JNK-induced MCP-1 production in spinal cord astrocytes contributes to central sensitization and neuropathic pain. J Neurosci 2009, 29: 4096–4108.
17. Zhou Y, Tang H, Xiong H. Chemokine CCL2 enhances NMDA receptor-mediated excitatory postsynaptic current in rat

hippocampal slices-a potential mechanism for HIV-1-associated neuropathy?. J Neuroimmune Pharmacol 2016, 11: 306–315.
18. Luscher C, Malenka RC. NMDA receptor-dependent long-term potentiation and long-term depression (LTP/LTD). Cold Spring Harb Perspect Biol 2012, 4.
19. Spiga S, Talani G, Mulas G, Licheri V, Fois GR, Muggironi G, *et al.* Hampered long-term depression and thin spine loss in the nucleus accumbens of ethanol-dependent rats. Proc Natl Acad Sci U S A 2014, 111: E3745-3754.
20. Chiou CS, Huang CC, Liang YC, Tsai YC, Hsu KS. Impairment of long-term depression in the anterior cingulate cortex of mice with bone cancer pain. Pain 2012, 153: 2097–2108.
21. Wei F, Li P, Zhuo M. Loss of synaptic depression in mammalian anterior cingulate cortex after amputation. J Neurosci 1999, 19: 9346–9354.
22. Zhang ZJ, Cao DL, Zhang X, Ji RR, Gao YJ. Chemokine contribution to neuropathic pain: respective induction of CXCL1 and CXCR2 in spinal cord astrocytes and neurons. Pain 2013, 154: 2185–2197.
23. Thomas MJ, Beurrier C, Bonci A, Malenka RC. Long-term depression in the nucleus accumbens: a neural correlate of behavioral sensitization to cocaine. Nat Neurosci 2001, 4: 1217–1223.
24. Baliki MN, Petre B, Torbey S, Herrmann KM, Huang L, Schnitzer TJ, *et al.* Corticostriatal functional connectivity predicts transition to chronic back pain. Nat Neurosci 2012, 15: 1117–1119.
25. Makary MM, Polosecki P, Cecchi GA, DeAraujo IE, Barron DS, Constable TR, *et al.* Loss of nucleus accumbens low-frequency fluctuations is a signature of chronic pain. Proc Natl Acad Sci U S A 2020, 117: 10015–10023.
26. Britt JP, Benaliouad F, McDevitt RA, Stuber GD, Wise RA, Bonci A. Synaptic and behavioral profile of multiple glutamatergic inputs to the nucleus accumbens. Neuron 2012, 76: 790–803.
27. Lee AT, Vogt D, Rubenstein JL, Sohal VS. A class of GABAergic neurons in the prefrontal cortex sends long-range projections to the nucleus accumbens and elicits acute avoidance behavior. J Neurosci 2014, 34: 11519–11525.
28. Taverna S, van Dongen YC, Groenewegen HJ, Pennartz CM. Direct physiological evidence for synaptic connectivity between medium-sized spiny neurons in rat nucleus accumbens in situ. J Neurophysiol 2004, 91: 1111–1121.
29. Burke DA, Rotstein HG, Alvarez VA. Striatal local circuitry: a new framework for lateral inhibition. Neuron 2017, 96: 267–284.
30. Duguid IC, Smart TG. Retrograde activation of presynaptic NMDA receptors enhances GABA release at cerebellar interneuron-Purkinje cell synapses. Nat Neurosci 2004, 7: 525–533.
31. Gubellini P, Ben-Ari Y, Gaiarsa JL. Endogenous neurotrophins are required for the induction of GABAergic long-term potentiation in the neonatal rat hippocampus. J Neurosci 2005, 25: 5796–5802.
32. Sivakumaran S, Mohajerani MH, Cherubini E. At immature mossy-fiber-CA3 synapses, correlated presynaptic and postsynaptic activity persistently enhances GABA release and network excitability *via* BDNF and cAMP-dependent PKA. J Neurosci 2009, 29: 2637–2647.
33. Liu D, Tang QQ, Yin C, Song Y, Liu Y, Yang JX, *et al.* Brain-derived neurotrophic factor-mediated projection-specific regulation of depressive-like and nociceptive behaviors in the mesolimbic reward circuitry. Pain 2018, 159: 175.
34. Zhang H, Qian YL, Li C, Liu D, Wang L, Wang XY, *et al.* Brain-derived neurotrophic factor in the mesolimbic reward circuitry mediates nociception in chronic neuropathic pain. Biol Psychiatry 2017, 82: 608–618.
35. Liu Y, Zhang LI, Tao HW. Heterosynaptic scaling of developing GABAergic synapses: dependence on glutamatergic input and developmental stage. J Neurosci 2007, 27: 5301–5312.
36. Chiu CQ, Martenson JS, Yamazaki M, Natsume R, Sakimura K, Tomita S, *et al.* Input-specific nmdar-dependent potentiation of dendritic gabaergic inhibition. Neuron 2018, 97(368–377): e363.
37. Spicarova D, Adamek P, Kalynovska N, Mrozkova P, Palecek J. TRPV1 receptor inhibition decreases CCL2-induced hyperalgesia. Neuropharmacology 2014, 81: 75–84.
38. D'Amour JA, Froemke RC. Inhibitory and excitatory spike-timing-dependent plasticity in the auditory cortex. Neuron 2015, 86: 514–528.
39. Luo C, Kuner T, Kuner R. Synaptic plasticity in pathological pain. Trends Neurosci 2014, 37: 343–355.
40. Deng PY, Lei S. Long-term depression in identified stellate neurons of juvenile rat entorhinal cortex. J Neurophysiol 2007, 97: 727–737.
41. Thomas MJ, Malenka RC, Bonci A. Modulation of long-term depression by dopamine in the mesolimbic system. J Neurosci 2000, 20: 5581–5586.
42. Liu L, Wong TP, Pozza MF, Lingenhoehl K, Wang Y, Sheng M, *et al.* Role of NMDA receptor subtypes in governing the direction of hippocampal synaptic plasticity. Science 2004, 304: 1021–1024.
43. Bie B, Brown DL, Naguib M. Synaptic plasticity and pain aversion. Eur J Pharmacol 2011, 667: 26–31.
44. Bliss TV, Collingridge GL, Kaang BK, Zhuo M. Synaptic plasticity in the anterior cingulate cortex in acute and chronic pain. Nat Rev Neurosci 2016, 17: 485–496.